Acta Crystallographica Section F
Structural Biology and Crystallization Communications
ISSN 1744-3091

Cloning, expression, purification, crystallization and preliminary X-ray diffraction analysis of DapB (Rv2773c) from *Mycobacterium tuberculosis*

Georgia Kefala, Robert Janowski, Santosh Panjikar, Christoph Mueller-Dieckmann and Manfred S. Weiss*

EMBL Hamburg Outstation, c/o DESY, Notkestrasse 85, D-22603 Hamburg, Germany

Correspondence e-mail: msweiss@embl-hamburg.de

Received 29 April 2005
Accepted 19 June 2005
Online 30 June 2005

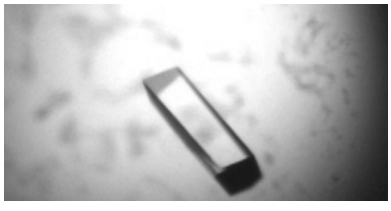

Dihydrodipicolinate reductase from *Mycobacterium tuberculosis* (DapB, DHDPR, Rv2773c) has been cloned and heterologously expressed in *Escherichia coli*, purified using standard chromatographic techniques and crystallized in three different crystal forms. Preliminary diffraction data analysis suggests the presence of two tetramers in the asymmetric unit of one crystal form and half a tetramer in the other two crystal forms.

1. Introduction

In both plants and bacteria, the biosynthesis of the amino acid L-lysine starts from L-aspartate. The first unique reaction in lysine biosynthesis is the condensation of pyruvic acid with aspartate semialdehyde, which is catalyzed by the enzyme dihydrodipicolinate synthase (DapA, DHDPS). The product of this reaction is the unstable cyclic imine 4-hydroxy-2,3,4,5-tetrahydrodipicolinic acid (Blickling *et al.*, 1997), which is believed to convert spontaneously to the α,β-unsaturated imine 2,3-dihydrodipicolinic acid. The next enzyme in the pathway, dihydrodipicolinate reductase (DapB, DHDPR), catalyses the subsequent pyridine nucleotide-dependent reduction of this imine to produce 2,3,4,5-tetrahydrodipicolinic acid. Since L-lysine is an essential amino acid for animals, the enzymes of this biosynthetic pathway have recently drawn increased attention as potential targets for new antibacterial drugs and herbicides (Hutton *et al.*, 2003).

DHDPR from *Escherichia coli* has been cloned (Bouvier *et al.*, 1984), purified and characterized kinetically (Reddy *et al.*, 1995). It is postulated that the enzymatic reaction proceeds in an ordered fashion, with NADH binding preceding substrate binding and product release preceding oxidized cofactor release. It has also been established that both NADH as well as NADPH can be utilized by the enzyme as cofactor.

The crystal structures of *E. coli* DHDPR complexed with NADH (Scapin *et al.*, 1995) and more recently of *Thermotoga maritima* DHDPR complexed with an NADH analogue (Joint Center for Structual Genomics, work to be published) have been determined. In addition, the ternary complexes of the enzyme with the inhibitor 2,6-pyridinedicarboxylate (2,6-PDC) and the cofactors NADH and NADPH have also been studied for the *E. coli* (Scapin *et al.*, 1997) and the *Mycobacterium tuberculosis* systems (Cirilli *et al.*, 2003). In all cases, DHDPR occurs as a homotetramer exhibiting 222 symmetry. Each of the four subunits consists of two domains connected by two hinge regions. The N-terminal domain is involved in cofactor binding, while the C-terminal domain is responsible for substrate binding and tetramerization. More precisely, Cirilli *et al.* (2003) define the N-terminal domain of *M. tuberculosis* DHDPR as composed of residues 1–106 and 216–245 and the C-terminal domain as composed of residues 107–215. This means that the C-terminal domain is really an insertion in the N-terminal domain. In the NADH complex of *E. coli* DHDPR one of the four subunits is unliganded and adopts an open conformation, while the three other subunits are complexed with NADH and inhibitor and adopt a closed conformation. This suggests that DHDPR undergoes a major conformational change upon binding of substrate (or inhibitor) and cofactor. Therefore, the structures of the apoenzyme as well as of the complex with only

cofactor or inhibitor will shed further light on the mechanism of function of the enzyme. Here, we report the crystallization of the apoenzyme and of the NADH complex of *M. tuberculosis* DHDPR in three different crystal forms and a preliminary X-ray diffraction investigation of these crystal forms.

2. Experimental methods

2.1. Cloning

Genomic DNA from the H37Rv strain of *M. tuberculosis* was used as a template for the polymerase chain reaction. Two constructs were prepared. The first construct (DapB construct 1) was designed for cloning in the pET22b vector (Novagen) and thus contained 5′-*Nde*I and 3′-*Xho*I restriction sites (in bold) and an additional thrombin-cleavage site (underlined) before the C-terminal His_6 tag. The following two primers (Invitrogen) were designed: 5′-GGGGCATATGGCTCGGGTAGGCGTCCTTGGAGCCAAAGGCAAGG-3′ and 5′-GGGG**CTCGAG**ACCTCGTGGTACACCGTGCAGATCGAGTAGGGGCTCAAGACCTACGGTGAG-3′. The GCT triplet coding for Ala was introduced as the second codon to increase the efficiency of expression (Looman *et al.*, 1987). For the second construct (DapB construct 2) the following two oligonucleotide primers were used for the amplification (MWG Biotech): 5′-AAAA**CCATGG**CTCGGGTAGGCGTCCTTGGAGCCAAAGGCAAGG-3′ and 5′-AAAA**CTCGAG**TTAGTGCAGATCGAGTAGGGGCTCAAGACCTACGGTGAG-3′ as forward and reverse primers, respectively. In the forward primer the additional underlined bases were introduced to place the gene in the frame for transcription. Therefore, the protein product contains an extra Ala residue at position 2 (codon GCT). The amplified fragment containing 5′-*Nco*I and 3′-*Xho*I restriction sites (shown in bold in the primer sequence) was digested and ligated to the pETM-11 expression vector, downstream of the sequence coding for the N-terminal His_6 tag and the recombinant tobacco etch virus protease (TEV) cleavage site. Both constructs were sequenced to confirm the cloning of the *dapB* gene sequence in the frame.

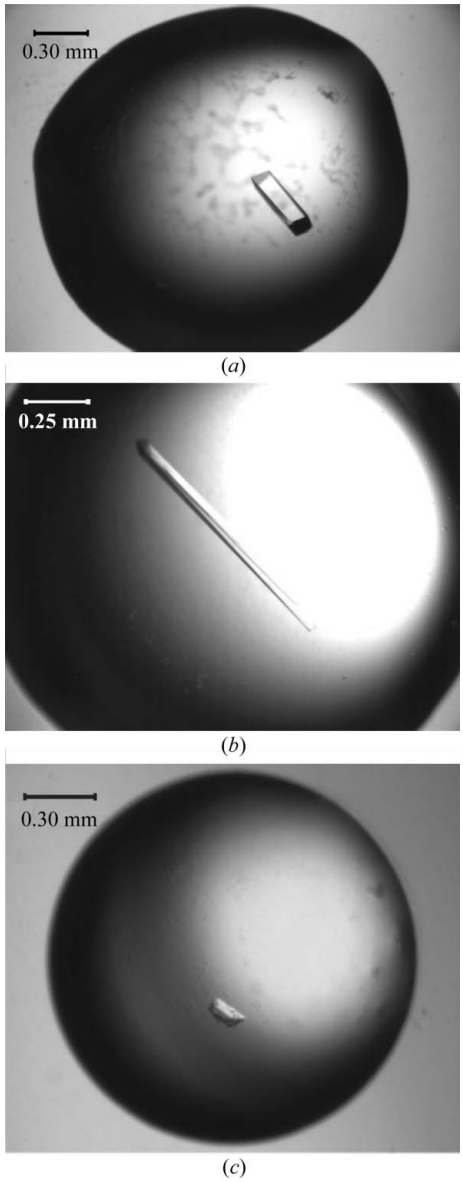

Figure 1
Images of crystallization experiments for the three crystal forms of *M. tuberculosis* DapB. (*a*) Crystal form *A*; (*b*) crystal form *B*; (*c*) crystal form *C*.

2.2. Expression and Purification

The recombinant plasmids were used to transform *E. coli* BL21-CodonPlus(DE3)-RP cells (Stratagene). Cells from an overnight 5 ml pre-culture were grown in LB broth medium containing chloramphenicol (30 µg ml^{-1}) at a temperature of 310 K and shaken at 200 rev min^{-1}. For the DapB construct 1 (in the pET22b vector) 50 µg ml^{-1} carbenicillin was added, while for the DapB construct 2 (in the pETM-11 vector) 30 µg ml^{-1} kanamycin was added. The culture was induced with 0.25 m*M* isopropyl-*β*-D-thiogalactopyranoside (IPTG) at an OD_{600} of approximately 0.6 at 293 K. Following induction, the culture was incubated for about 15 h at 293 K and 220 rev min^{-1} and was then harvested. The cells were frozen and stored at 193 K until further processing. 1 g cell pellet was dissolved in 10 ml buffer *A* [20 m*M* Tris pH 8.0, 250 m*M* NaCl, 10 m*M* imidazole, 5%(*v*/*v*) glycerol] and one Complete Mini EDTA-free Protease Inhibitor Cocktail tablet (Roche) per 30 ml and then lysed by sonication for 3 × 5 min in 0.3 s pulses at 277 K. The cell debris was pelleted by centrifugation for 60 min at 277 K and 20 000 rev min^{-1}. The crude lysate was filtered through a 0.22 µm membrane and was loaded onto a 5 ml Hi-Trap Chelating HP column charged and equilibrated with Ni^{2+} and buffer *A*, respectively. In order to remove unbound proteins, the column was first washed with five column volumes of buffer *A*, then with five column volumes of buffer *B* [20 m*M* Tris pH 8.0, 1 *M* NaCl, 10 m*M* imidazole, 5%(*v*/*v*) glycerol, 2 m*M* *β*-ME] and finally with five column volumes of buffer *C* [20 m*M* Tris pH 8.0, 250 m*M* NaCl, 50 m*M* imidazole, 5%(*v*/*v*) glycerol]. The protein was eluted by running a linear gradient from 50 to 800 m*M* imidazole (in buffer *C*). The major peak fractions were pooled and dialyzed against buffer *D* [20 m*M* Tris pH 8.0, 250 m*M* NaCl, 5%(*v*/*v*) glycerol]. During overnight dialysis at 277 K, the His tag was cleaved off the protein produced from the pETM-11 construct by adding TEV protease. The cleaved and dialyzed protein solution was passed through a Hi-Trap Chelating HP column pre-equilibrated with buffer *D* and recovered in the flowthrough. Attempts to cleave the C-terminal His tag from the protein produced from the pET22b construct using thrombin were not successful. The protein was subsequently purified by gel filtration (Superdex 200, 16/60) using buffer *D* for both equilibration and elution. The protein eluted with an apparent molecular weight of approximately 100 kDa, which is consistent with a homotetramer. The peak fractions were analyzed by SDS–PAGE, pooled and concentrated to 15 mg ml^{-1}.

Both columns used for purification were supplied by Amersham Pharmacia Biotech. The purity of the protein was then gauged by SDS–PAGE and its monodispersity by dynamic light scattering.

2.3. Crystallization

DapB construct 2 containing the additional two amino acids Gly and Ala at the N-terminus and an additional Ala after the first Met residue was crystallized using the hanging-drop vapour-diffusion method (1 µl protein solution and 1 µl reservoir solution) in the presence of 20–24%(*w*/*v*) PEG 3350, 120–140 m*M* $MgCl_2$, 100 m*M* Tris–HCl pH 8.5. Small thin plates appeared, which were then crushed and used for streak-seeding experiments. This led to the growth of larger single crystals (crystal form *A*; Fig. 1*a*), which could be used for data collection and which diffracted X-rays to about 2.3 Å resolution.

DapB construct 1 still containing the thrombin-cleavage site and the C-terminal His_6 tag was crystallized under the same conditions as described for crystal form *A* above. The crystals typically grew within a week to a maximum size of 300 µm (crystal form *C*; Fig. 1*c*). They diffracted X-rays to better than 2.5 Å resolution, albeit very anisotropically. Co-crystallization with the cofactor NADH was achieved by incubating the protein with 3 m*M* NADH for 30 min on ice prior to crystallization.

The addition of 4%(*v*/*v*) 1,3-propanediol to the crystallization conditions described above for DapB construct 1 led to the growth of rod-shaped crystals up to 1 mm in length (crystal form *B*; Fig. 1*b*), which diffracted X-rays to about 3.0 Å resolution.

2.4. Diffraction data collection and processing

Prior to data collection, all crystals were treated with cryoprotectant [20%(*v*/*v*) MPD in reservoir solution] and flash-cooled to 100 K. Diffraction data were then collected on the XRD beamline at ELETTRA (Trieste, Italy) for crystal forms *A* and *B* and on the X13 beamline (EMBL Hamburg, Germany) for crystal form *C* using a MAR CCD detector in all cases. The data were indexed and integrated using *DENZO* (Otwinowski & Minor, 1997) and scaled using *SCALEPACK* (Otwinowski & Minor, 1997). The redundancy-independent merging *R* factor $R_{\rm r.i.m.}$ and the precision-indicating merging *R* factor $R_{\rm p.i.m.}$ (Weiss, 2001) were calculated using the program *RMERGE* (available from http://www.embl-hamburg.de/~msweiss/projects/msw_qual.html or from MSW upon request). The relevant data-collection and processing parameters are given in Table 1. Intensities were converted to structure-factor amplitudes using the program *TRUNCATE* (French & Wilson, 1978; Collaborative Computational Project, Number 4, 1994).

Table 1
Data-collection and processing statistics.

Values in parentheses are for the last resolution shell.

	Crystal form		
	A	*B*	*C*
No. of crystals	1	1	1
Wavelength (Å)	1.100	1.000	0.804
Crystal-to-detector distance (mm)	150	210	220/300
Total rotation range (°)	200	140	269 + 200
Resolution range (Å)	99.0–2.30 (2.34–2.30)	99.0–2.90 (2.95–2.90)	99.0–2.34 (2.38–2.34)
Space group	$P2_12_12$	$P2_12_12$	$C2$
Unit-cell parameters (Å, °)	*a* = 59.26, *b* = 122.00, *c* = 77.93	*a* = 87.13, *b* = 89.46, *c* = 77.53	*a* = 238.60, *b* = 67.52, *c* = 154.49, β = 117.08
Mosaicity (°)	1.05	1.35	0.53
Total No. of reflections	174935	71353	462614
Unique reflections	25725	13836	80393
Redundancy	6.8	5.2	5.8
$I/\sigma(I)$	17.1 (1.8)	23.9 (4.0)	18.7 (3.3)
Completeness (%)	99.6 (99.1)	98.9 (99.8)	86.6 (76.6)
$R_{\rm merge}$ (%)	8.5 (73.4)	6.1 (50.4)	9.2 (30.1)
$R_{\rm r.i.m.}$ (%)	9.2 (82.2)	6.9 (56.1)	10.0 (35.4)
$R_{\rm p.i.m.}$ (%)	3.4 (35.8)	3.0 (24.3)	3.8 (18.2)
Overall *B* factor from Wilson plot (Å^2)	59.6	78.0	47.0
Optical resolution (Å)	1.87	2.15	1.80

3. Results and discussion

For one crystal of crystal form *A*, a complete X-ray diffraction data set was collected to 2.30 Å resolution (Table 1). The crystals belong to the orthorhombic space group $P2_12_12$. Packing considerations and a self-rotation function calculation suggest the presence of two subunits per asymmetric unit. Since it is likely that DapB crystallizes as a tetramer, the crystallographic twofold along the *c* axis would constitute one of the twofold axes contained in the homotetramer.

A form *B* crystal was also used for X-ray data collection. Although the crystal was highly mosaic (Table 1), it was possible to obtain a good and complete data set to 2.90 Å resolution. Surprisingly, the crystal belonged to the same space group as the crystal described in the previous paragraph, but exhibited two very different unit-cell parameters. Only the *c* axes seem to be identical. For the *a* and *b* axes there is no obvious way to relate the unit cell to that observed for form *A*. However, the cell volumes of both unit cells are similar and the self-rotation functions of both data sets look similar (data not shown); thus, it is likely that in this case the content of the asymmetric unit is also two subunits. This means that some relationship between the packing of the molecules must exist.

For crystal form *C*, only a crystal obtained in the presence of NADH was analysed by X-ray diffraction. A data set extending to 2.34 Å resolution was collected. However, the crystal exhibited very high anisotropy in its diffraction power. This explains the lower completeness of the data set (Table 1). In one direction of reciprocal space the data had to be cut to as low as 3.4 Å, whereas in the other two directions the data extended to the maximum resolution. The crystal belongs to the space group *C*2 and probably contains eight subunits, *i.e.* two tetramers, in the asymmetric unit.

None of the space groups and packing modes observed in the three crystal forms here have been observed before. DapB from *M. tuberculosis* has previously been crystallized as a ternary complex with NADH (or NADPH) and the inhibitor PDC, but the observed space group was $I2_12_12_1$ with two subunits per asymmetric unit. It is likely that the different complexation states primarily resulted in the different crystallization conditions. However, attempts to reproduce the published crystallization conditions for the ternary complexes using the DapB constructs described here failed. Thus, some of the differences must also be attributed to the different constructs (Cirilli *et al.*, 2003) and/or to the different purification schemes (Reddy *et al.*, 1995).

In summary, DapB from *M. tuberculosis* has been crystallized in three new and different crystal forms, each suitable for structure determination by X-ray crystallography. Since neither the apoenzyme nor the binary NADH complex of the *M. tuberculosis* have been observed previously, the structures of the enzyme in all three crystal forms and comparison with published structures will certainly shed further light on the flexibility and the mechanism of function of the enzyme.

We would like to thank Dr Jeanne Perry (UCLA) for providing genomic Mtb-DNA, the TB consortium (http://www.doe-mbi.ucla.edu/

TB) for postdoctoral exchange grants to GK and the X-Mtb consortium (http://www.xmtb.org) for funding through BMBF/PTJ grant No. BIO/0312992A. We would also like to acknowledge the staff of the ELETTRA synchrotron (Trieste, Italy) for data-collection time and the support by the EC Fifth Framework Programme 'Transnational Access to Major Research Infrastructures' (Contract No. HPRI-CT-1999-00033). CMD is a postdoctoral fellow funded by the Deutsche Forschungsgemeinschaft (DFG grant WE2520/2 to MSW).

References

Blickling, S., Renner, C., Laber, B., Pohlenz, H. D., Holak, T. A. & Huber, R. (1997). *Biochemistry*, **36**, 24–33.
Bouvier, J., Richaud, C., Richaud, F., Patte, J. C. & Stragier, P. (1984). *J. Biol. Chem.* **259**, 14829–14834.
Cirilli, M., Zheng, R., Scapin, G. & Blanchard, J. S. (2003). *Biochemistry*, **42**, 10644–10650.
Collaborative Computational Project, Number 4 (1994). *Acta Cryst.* D**50**, 760–763.
French, G. S. & Wilson, K. S. (1978). *Acta Cryst.* A**34**, 517–525.
Hutton, C. A., Southwood, T. J. & Turner, J. J. (2003). *Mini Rev. Med. Chem.* **3**, 115–127.
Looman, A. C., Bodlaender, J., Comstock, L. J., Eaton, D., Jhurani, P., de Boer, H. A. & van Knippenberg, P. H. (1987). *EMBO J.* **6**, 2489–2492.
Otwinowski, Z. & Minor, W. (1997). *Methods Enzymol.* **276**, 307–326.
Reddy, S. G., Sacchettini, J. C. & Blanchard, J. S. (1995). *Biochemistry*, **34**, 3492–3501.
Scapin, G., Blanchard, J. S. & Sacchettini, J. C. (1995). *Biochemistry* **34**, 3502–3512.
Scapin, G., Reddy, S. G., Zheng, R. & Blanchard, J. S. (1997). *Biochemistry*, **36**, 15081–11588.
Weiss, M. S. (2001). *J. Appl. Cryst.* **34**, 130–135.